Int. J. Heat Mass Transfer. Vol. 31, No. 5, pp. 1081–1091, 1988
Printed in Great Britain

0017–9310/88 $3.00 + 0.00

Dispersion in cellular thermal convection in porous layers

JOHN G. GEORGIADIS† and I. CATTON
Department of Mechanical, Aerospace and Nuclear Engineering, University of California, Los Angeles, CA 90024, U.S.A.

(*Received* 30 *October* 1986 *and in final form* 15 *October* 1987)

Abstract—A numerical and experimental study is reported for the case of two-dimensional buoyancy-driven convection in saturated horizontal packed beds. The classical Darcy model is extended by the Forchheimer (inertial) term and the effective thermal conductivity of the medium is represented by the sum of a stagnant and a (hydrodynamic) dispersive component, the latter being proportional to the local filtration velocity amplitude. Bifurcation analysis of the porous Bénard problem with dispersive and inertial terms proves that the results of the classical Darcy model still hold at the onset of convection for weak dispersion. Both terms are important for steady convection in shallow packed beds. The effect of dispersion on Nusselt number is stronger than that of inertia unless the Prandtl number of the porous medium is of order 0.01 or less. The ratio of layer thickness to bead diameter is shown to be a significant parameter of the problem that can help explain some contradictory experimental results.

1. INTRODUCTION

ANALYSIS of buoyancy-driven convection in coarse porous layers—as exemplified by packed beds of spherical beads—is motivated by applications related to insulation or energy storage systems. Traditionally, a fluid-saturated packed bed is treated as a continuum if the layer thickness L is sufficiently larger than the bead diameter d. However, experiments by Close *et al.* [1] in shallow horizontal packed beds (small L/d ratio) indicated that the results of the continuum approach might be still valid near the onset of convection. In the present work, we assume that the continuum model holds and we simply compare its predictions with experiments. In the following, we will consider the problem of natural convection in a fully-saturated packed bed bounded by isothermal impervious horizontal surfaces of infinite extent with the lower surface being hotter than the upper. The system bifurcates from conduction to convection when a critical value of the temperature gradient is exceeded and this will be referred to as 'the porous Bénard problem'.

Careful analysis of the heat transfer measurements for the porous Bénard problem by Combarnous [2] and Close *et al.* [1] shows that the ratio L/d should be considered as an additional parameter of the problem and suggests the need to extend the classical Darcy formulation. The work of Neischloss and Dagan [3] for natural convection and of Rubin [4] for forced convection are early attempts to accomplish this by considering the augmentation of the effective heat conductivity due to hydrodynamic dispersion. Although the two analytical works mentioned above employed different dispersivity models, they both predicted a reduction of the heat transport through the layer as the ratio L/d decreases. Based on heat transfer experiments in beds containing 2–5 layers of polypropylene beads, Close *et al.* [1] reached the same conclusion but suggested that this reduction is an inertial effect. They pointed out that their Nusselt number data for 5 layers ($L/d = 3.87$) lie below the Nusselt number data of Combarnous [2] for water-saturated beds consisting of 17 layers of polypropylene beads ($L/d = 13.37$). An inconsistency is revealed if we examine the two sets of Nusselt number measurements by Combarnous [2] for water-saturated beds (of constant thickness) obtained for two sizes of glass beads $d = 4$ and 1.7 mm; the Nusselt numbers for the former lie above the ones for the latter. The same trend is also verified for the water-saturated beds of quartz beads.

Kvernvold and Tyvand [5] solved numerically the porous Bénard problem employing the same dispersion model as Neischloss and Dagan [3] and found that, although for small Rayleigh numbers the heat transport decreases with decreasing L/d (same as the result of Neischloss and Dagan [3]), for larger Rayleigh numbers the opposite happens. An attempt to reduce the scatter in the Nu vs Ra_m data in the literature was reported by Prasad *et al.* [6] who used a constant effective conductivity that is a function of the convective state (Ra_m) and of the physical properties of the medium. They implemented an iterative implicit scheme to compute this effective conductivity in terms of existing experimental Nusselt number data, but no physical mechanism was provided to justify the specific formula for the conductivity, as

† Present address: Department of Mechanical Engineering and Materials Science, Duke University, Durham, NC 27706, U.S.A.

NOMENCLATURE

a_m	thermal diffusivity of the medium, $k_m/(\rho c)_f$ [$m^2 s^{-1}$]
A_0, A_k	Fourier coefficients of the velocity amplitude, equation (13d)
b	inertial resistance coefficient in equation (5) [m]
c	specific heat [$J kg^{-1} K^{-1}$]
C	dispersion coefficient, equation (7)
d	spherical bead diameter [m]
D^*	ratio of dispersive to stagnant conductivity, equation (3)
Da	Darcy number, γ/L^2
Di	dispersivity in equation (7), $Cd/L(1-\phi)$
g	gravitational acceleration in the z-direction [$m s^{-2}$]
k^*	effective thermal conductivity of the medium, equation (6) [$W m^{-1} K^{-1}$]
k_m	stagnant thermal conductivity of the fluid–solid medium, equation (6) [$W m^{-1} K^{-1}$]
K	total number of Fourier modes in the y-direction
L	thickness of the porous layer [m]
Nu	Nusselt number, equation (15)
P	average pressure of the interstitial fluid
Pe	Peclet number, $\lvert\mathbf{q}'\rvert(d/a_f)(1-\phi)^{-1} = \lvert\mathbf{q}\rvert(d/L)(k_m/k_f)(1-\phi)^{-1}$
Pr_m	Prandtl number of the medium, $\nu(\rho c)_f/k_m$
$\mathbf{q}$	dimensionless Darcy superficial velocity
Ra	Rayleigh number, $g\beta\Delta TL^3/(\nu a_m)$
Ra_m	porous Rayleigh number, $Da\,Ra$
t	time [s]
T	dimensionless temperature $(T'-T'_C)/\Delta T$
ΔT	temperature difference, $T'_H - T'_C$ [K]
v, w	horizontal, vertical velocity components, respectively
y, z	horizontal, vertical Cartesian coordinates, respectively.

Greek symbols

α	dimensionless wave number, $2\pi/\lambda$
β	volumetric thermal expansion coefficient of the fluid [K^{-1}]
γ	porous medium permeability [m^2]
θ	dimensionless temperature perturbation
ν	kinematic viscosity [$m^2 s^{-1}$]
ρ	density [$kg m^{-3}$]
ϕ	porosity
ω	inertial drag coefficient, $bL/\gamma\, Pr_m$.

Subscripts

C	cold
f	fluid
H	hot
k	kth order
m	porous medium
0	horizontal average, zeroth order.

Superscripts

c	critical value
′	dimensional.

Special symbols

D	z-derivative
$\langle . \rangle$	volume average over the flow domain
$O(.)$	order of magnitude.

Close [7] pointed out. When some data for low L/d values still diverged, it was postulated that the Darcy law fails (Fig. 18 in the paper of Prasad *et al.* [6]).

Georgiadis and Catton [8] included the inertial (Forchheimer) term in the momentum equation and used the measured values of the stagnant effective conductivity in the energy equation. Their numerical predictions of the heat transfer reproduce the large-scale scatter of the Nu vs Ra_m data of Jonsson and Catton [9] for the porous Bénard problem. According to the above model, the inertial effect (its relative importance being expressed by the parameter $\omega\, Da$ that is proportional to $d/L\, Pr_m$) diminishes the net heat transfer. Hence, the Nusselt number predictions of the classical Darcy model ($\omega = 0$) should be the upper bound. However, the Nu measured by Combarnous [2] for natural convection in polypropylene packed beds saturated with water or oil exceed the maximum Nu of the Darcy model (obtained by using the wave number that maximizes Nu). In view of the contradictory (i.e. non-monotonic) behavior of the Nu vs L/d results found in the literature, it is obvious that another physical mechanism has to be taken into account in combination with inertia. The enhancement of conductivity due to dispersion is a likely candidate. Both inertia and dispersive effects have been previously considered by Rubin [4] for forced convection, by Cheng and Zheng [10] for mixed convection boundary-layer flow, and by Hong and Tien [11] for vertical-plate natural convection in porous media.

The mission of the present work is to demonstrate the role of dispersion on heat transport when the boundary-layer approximation is not applicable and the Forchheimer formulation is adopted for natural convection in porous media. A canonical problem is chosen for this purpose (the porous Bénard problem). The way in which the dispersive component enters the formulation is explained in Section 2 and the non-Darcian effects on the onset of convection are studied by performing a simple bifurcation analysis in Section 3. The numerical algorithm is developed in Section 4

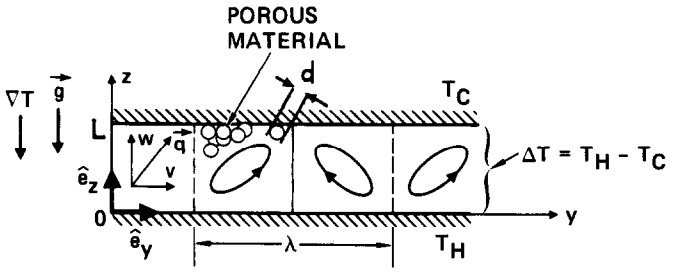

FIG. 1. The porous Bénard problem: natural convection in a fully-saturated packed bed bounded by isothermal impervious horizontal surfaces of infinite extent with the lower surface being hotter than the upper.

and its convergence is checked. Finally, the numerical solution is compared to experiments in Section 5 and a summary of the concluding remarks is presented in Section 6. This is a companion to the paper by Georgiadis and Catton [8].

2. FORMULATION OF THE PROBLEM

The flow domain of the porous Bénard problem is shown in Fig. 1. The packed bed is fully saturated with a Boussinesq incompressible fluid. The heterogeneous system fluid–solid matrix is regarded as a continuous medium on the Darcy scale. Thus, we assume that the convective motion of the interstitial fluid in the fully-saturated packed bed is governed by the following equations in non-dimensional form:

$$\nabla \cdot \mathbf{q} = 0 \tag{1}$$

$$\frac{1}{\phi Pr_m}\frac{\partial \mathbf{q}}{\partial t} = -\nabla P + Ra\, T\hat{\mathbf{e}}_z - \frac{1}{Da}\mathbf{q} - \omega|\mathbf{q}|\mathbf{q} \tag{2}$$

$$\frac{(\rho c)_m}{(\rho c)_f}\frac{\partial T}{\partial t} = -\mathbf{q}\cdot\nabla T + \nabla\cdot[(1+D^*)\nabla T] \tag{3}$$

where length, velocity, pressure, temperature are scaled with L, a_m/L, $\rho v a_m/L^2$, ΔT, respectively, P the local interstitial pressure minus the hydrostatic component, and T the local temperature minus the cold wall temperature T_C. The governing equations, equations (1)–(3), are supplemented by the following boundary conditions:

$$\begin{aligned} &\mathbf{q}\cdot\hat{\mathbf{e}}_z = 0,\ T = 1 \quad \text{at} \quad z = 0;\\ &\mathbf{q}\cdot\hat{\mathbf{e}}_z = 0,\ T = 0 \quad \text{at} \quad z = 1. \end{aligned} \tag{4}$$

The following standard empirical relations are used to give the permeability and inertial resistance coefficient, cf. Georgiadis and Catton [8]:

$$\gamma = \frac{d^2\phi^3}{150(1-\phi)^2}, \quad b = \frac{1.75d}{150(1-\phi)}. \tag{5}$$

We cannot avoid mentioning that the correct formulation of the problem of convection through porous media remains a point of major contention in the literature. Concerning the momentum equation, many researchers are in favor of the following 'full' form [12]:

$$\frac{1}{\phi Pr_m}\left[\frac{\partial \mathbf{q}}{\partial t} + \mathbf{q}\cdot\nabla\mathbf{q}\right] = -\nabla P + Ra\, T\hat{\mathbf{e}}_z - \frac{1}{Da}\mathbf{q} - \omega|\mathbf{q}|\mathbf{q} + \frac{1}{\phi}\nabla^2\mathbf{q}.$$

Let us present our arguments for reducing the equation above to equation (2). There is no controversy concerning the Darcian drag term (third term on the right-hand side). For the Bénard problem, the last term on the right-hand side of the above equation (Brinkman's extension) has been proven to have a negligible effect on the onset of cellular convection if $Da < 10^{-3}$. In our computations, the maximum value of Da remains close to 10^{-3}. The magnitude of Da expresses the ratio (Brinkman term)/(Darcy drag) away from the solid boundaries. Near these boundaries, the Brinkman term is significant because the shear increases to accommodate the no-slip condition. The latter condition is entirely empirical and has been introduced for convenience. An additional complication of the problem of imposing the proper boundary conditions (at the interface between the packed bed and the wall) is introduced by the porosity variation due to the presence of solid walls. This induces higher velocities near the boundaries (channelling phenomenon) which, based on the analysis of Hong *et al.* [13] enhances the Nusselt number. We performed some preliminary computations for the Bénard problem with a variable porosity model and our results indicated that the relative increase of the Nusselt number due to porosity variation near the walls is almost balanced by the decrease of Nu predicted by the Brinkman-extended model. It makes sense that, had we chosen to introduce the Brinkman extension in equation (2), we would have to account for the porosity variation near the walls (especially for the coarse packed beds) in order to be consistent. Its theoretical justification pending, Brinkman's term is dropped and we consider here the case of a constant porosity medium. The slip condition is imposed at the solid walls. The magnitude of the Forchheimer quadratic inertial term in the 'full' equation (fourth term on the right-hand side) is of order $1.75(L/d)(1-\phi)\phi^{-2}$ with respect to the convective inertial term. Therefore, the latter can be neglected even

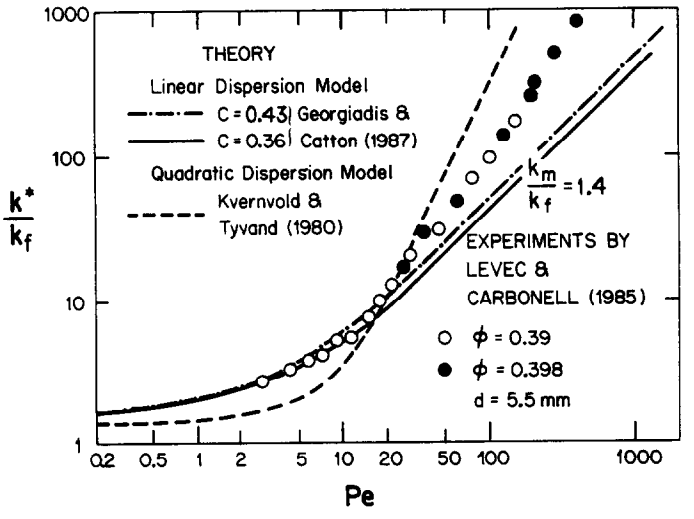

FIG. 2. Effective axial thermal conductivity in packed beds.

for the coarse packed beds considered in Section 5.

It is plausible to assume that there are no steep temperature gradients in natural convection and that the convective velocities are sufficiently slow for the range of Rayleigh numbers considered. Consequently, local thermodynamic equilibrium prevails, cf. Whitaker [14], and we postulate that the one-equation model (3) can accurately describe the heat transfer process in the homogenized porous medium. The form of the energy equation (3) was derived by Georgiadis and Catton [15] for steady-state heat transport in a steady isotropic interstitial field. The appearance of D^* in the heat transport coefficient in equation (3) represents the enhancement of the heat transfer that is caused by the hydrodynamic mixing (dispersion) of the interstitial fluid at the pore scale. According to the stochastic phenomenological model developed by Georgiadis and Catton [15] for isotropic porous media, the 'effective' heat conduction coefficient can be written in the form

$$\frac{k^*}{k_f} = \frac{k_m}{k_f} + C\,Pe \tag{6}$$

where k_m is the (stagnant) value of the effective conductivity of the system porous matrix–fluid in the absence of convection. Due to equation (6), the dimensionless dispersive conductivity component in equation (3) becomes

$$D^* = \frac{C}{1-\phi}\frac{d}{L}|\mathbf{q}| = Di|\mathbf{q}|. \tag{7}$$

In principle, the value of the dispersion coefficient C in equations (6) and (7) depends on the type of packing of the bed. For a certain type of Gaussian packing [16] and $\phi = 0.39$, our model gives $C = 0.43$, and this seems to underpredict (for the range $Pe > 20$) the values of the effective axial conductivity measured by Levec and Carbonell [17] under transient conditions (Fig. 2). The aforementioned discrepancy can be attributed to the transient heat exchange contribution to the apparent transport coefficient. Georgiadis and Catton [15] proved that, by adding this contribution—as estimated by Levec and Carbonell [17]—to expression (7), a realistic estimate of the effective axial transport coefficient under transient conditions is obtained that agrees with measurements for the whole range of Peclet numbers. Therefore, expressions (6) and (7) remain valid for steady-transport through packed beds irrespective of the Peclet number. We decided to perform our calculations with the value $C = 0.36$, which gives the best fit of the data obtained by Levec and Carbonell [17] for the range $0 \leqslant Pe \leqslant 20$ as shown in Fig. 2. This includes the range of Peclet numbers ($0 < Pe < 10$) encountered in natural convection for the range of Rayleigh numbers that we considered during the course of our computations. For comparison, we also plot in Fig. 2 the curve corresponding to the quadratic dispersion model used by Kvernvold and Tyvand [5] which clearly underpredicts the data for approximately the same range of Peclet numbers. The quadratic dispersion model was based on the analytical work of Saffman [18] who suggested a quadratic dependence of the effective transport coefficient on velocity for asymptotically small Peclet numbers.

3. ONSET OF CONVECTION: BIFURCATION ANALYSIS

The basic solution of equations (1)–(4) is the conductive state

$$\mathbf{q}_b = 0, \quad T_b = 1 - z.$$

Following the formulation of Joseph [19], we set $\mathscr{R} = Ra_m^{1/2}$, rescale $\theta = \mathscr{R}(T - T_b)$, and derive the following perturbation equations from equations (1)–(4) and (7):

$$\frac{Da}{\phi\, Pr_m}\frac{\partial \mathbf{q}}{\partial t}+\mathbf{q}-\mathscr{R}\theta\hat{\mathbf{e}}_z+\omega\, Da|\mathbf{q}|\mathbf{q}=-Da\nabla P \quad (8a)$$

$$\frac{(\rho c)_m}{(\rho c)_f}\frac{\partial \theta}{\partial t}+\mathbf{q}\cdot\nabla\theta-\mathscr{R}w-\nabla^2\theta - Di\nabla\cdot\{|\mathbf{q}|(\nabla\theta-\mathscr{R}\hat{\mathbf{e}}_z)\}=0 \quad (8b)$$

$$(\mathbf{q},\theta)\in\mathscr{I},\quad \mathscr{I}=[\mathbf{q},\theta:\nabla\cdot\mathbf{q}=0 \text{ in } \Omega,\ \mathbf{q}\cdot\mathbf{n}=0 \text{ on } \partial\Omega,\ \mathbf{n}\cdot\nabla\theta=0 \text{ on } S,\ \theta=0 \text{ on } z=0,1] \quad (8c)$$

where $\partial\Omega$ is the boundary of the flow domain, $\mathbf{n}$ its unit normal vector and S the lateral boundary which is assumed to be insulated. In order to reconcile our assumption of the laterally unbounded porous layer with the existence of a 'slip' lateral surface S, we can identify the latter with the vertical boundary enclosing a pair of counterrotating rolls of width λ (Fig. 1). Such a cellular form appears after the onset of the convective motion as we will show in the next paragraph. The corresponding two-dimensional (y, z) flow domain is $\Omega=[0,\lambda]\times[0,1]$.

Denoting by $\mathbf{Q}$ the four-component vector with components $(\mathbf{q},\theta)$, the bifurcation problem (8) can be written in matrix form

$$\mathbf{L}\cdot\mathbf{Q}+\mathbf{N}(\mathbf{Q})=-Da\nabla p;\quad \mathbf{Q}\in\mathscr{I} \quad (9)$$

where $\mathbf{L}$ and $\mathbf{N}$ are 4×4 matrix linear and non-linear operators, respectively. We try a double expansion in terms of the classical bifurcation parameter ε and Di. There is no power series in ε because $|\mathbf{q}|$ (which appears in the non-Darcian terms of equations (8a) and (8b)) is not analytic. It is probably valid to assume [20] that

$$\mathscr{R}(\varepsilon, Di)=\mathscr{R}_0+\varepsilon\mathscr{R}_1+Di\,\mathscr{R}_2+o(\varepsilon, Di) \quad (10a)$$

$$\mathbf{Q}(\varepsilon, Di)=\varepsilon\mathbf{Q}_0+\varepsilon^2\mathbf{Q}_1+\varepsilon Di\mathbf{Q}_2+o(\varepsilon^2, \varepsilon Di) \quad (10b)$$

where $\mathbf{Q}_0$ is the solution of equation (9) that bifurcates from the basic state (conduction) when $\mathscr{R}(\varepsilon=0)=\mathscr{R}_0$. Inserting expansion (10) into equation (9), imposing boundary condition (8c), and following the procedure outlined in Section 76 of Joseph [19], we obtain

$$O(\varepsilon):\quad \mathscr{R}_0\langle w_0\theta_0\rangle=\langle|\mathbf{q}_0|^2\rangle \quad (11a)$$

$$O(\varepsilon^2):\quad 2\mathscr{R}_1\langle w_0\theta_0\rangle=\left\{\omega\, Da\langle|\mathbf{q}_0|^3\rangle\right\}\frac{\varepsilon}{|\varepsilon|} \quad (11b)$$

$$O(\varepsilon\, Di):\quad \mathscr{R}_2=0 \quad (11c)$$

where w_0 is the z-component of $\mathbf{q}_0$ and $(\mathbf{q}_0,\theta_0)$ are the components of $\mathbf{Q}_0$. The angular brackets designate the volume-averaged integral defined on the flow domain Ω. The lowest order problem $(O(\varepsilon))$, which is the spectral problem for the stability of the conduction solution (basic state) of equations (1)–(3), is identical to the zeroth order problem in the Darcy porous Bénard formulation (no inertia or dispersion terms), cf. Joseph [19]. Consequently, this spectral problem has a simple real eigenvalue (zero), convection starts in the form of two-dimensional rolls, and the critical parameters corresponding to the onset of convection are

$$\mathscr{R}_0=\sqrt{Ra_m^c}=2\pi,\quad \alpha^c=\pi. \quad (12)$$

Equation (11a) is the energy identity obtained for $\varepsilon=0$ by multiplying the momentum equation (8a) by $\mathbf{q}$ and averaging over Ω. From equations (12) and (11a) we deduce that $\langle w_0\theta_0\rangle$ is positive definite. Equations (11b) and (11c) are the solvability conditions (section 76 of Joseph [19]). As a result of the existence of non-analytical terms in equations (8), $\mathscr{R}_1$ is not unique but reverses its sign around $\varepsilon=0$. Since $(\mathbf{q}_0,\theta_0)$ are uniquely defined, equations (11a) and (11b) imply that $\varepsilon\mathscr{R}_1$ is proportional to $|\varepsilon|$. Equation (11c) implies that the contribution of dispersion to the onset of convection is null, correct to $O(Di)$. Hence, the bifurcation curve $\mathscr{R}$ has a vertex at $\mathscr{R}_0$ and two symmetric *supercritical* bifurcation branches. This result has also been reported by Nield and Joseph [21] for the special case $Di=0$.

We have shown that, for weak dispersion ($Di\ll1$), neither the Forchheimer term nor the dispersion contribution influence the onset of convective motion as defined by equations (12). This has been verified (within experimental error) by Close *et al.* [1] even for the case of very coarse packed beds (low L/d ratio) such as the one consisting of only two layers of spherical beads. The insensitivity of the critical convection parameters of the porous Bénard problem to dispersion has also been proven by Neischloss and Dagan [3] for the quadratic dispersion model suggested by Saffman [18]. Employing the same model, Kvernvold and Tyvand [5] went further and delineated the linear stability regime for two-dimensional convection. According to their calculations, dispersion ($D^*\neq0$) extends the stability 'balloon' and thus the flow remains stable to cross-roll instabilities for Rayleigh numbers larger than the ones predicted by the classical Darcy model.

4. NUMERICAL SOLUTION OF FINITE AMPLITUDE TWO-DIMENSIONAL CONVECTION

Based on our conclusion in the previous section that convection in the porous Bénard problem is initiated in the form of straight horizontal rolls, we seek a steady two-dimensional solution of equations (1)–(4) in terms of the following Fourier expansions which have been truncated to K terms:

$$v(y,z)\simeq\sqrt{2}\sum_{k=1}^{K}v_k(z)\sin\alpha_k y \quad (13a)$$

$$w(y,z)\simeq\sqrt{2}\sum_{k=1}^{K}w_k(z)\cos\alpha_k y \quad (13b)$$

$$T(y,z)\simeq T_0(z)+\sqrt{2}\sum_{k=1}^{K}T_k(z)\cos\alpha_k y \quad (13c)$$

$$|\mathbf{q}| = \sqrt{(|w^2+v^2|)} \simeq \sqrt{2}A_0(z) + \sqrt{2}\sum_{k=1}^{K} A_k(z)\cos\alpha_k y \quad (13d)$$

where $\alpha_k = k\alpha$. By substituting equations (13) into equations (1)–(3), eliminating the pressure, and weighting and integrating over the wavelength, we obtain the weak formulation of the problem as a system of Galerkin ODEs

$$\alpha_k v_k + \mathrm{D}w_k = 0 \quad (14a)$$

$$\frac{1}{Da}(\mathrm{D}^2-\alpha^2)w_k + \alpha_k^2 Ra\, T_k = \omega(\alpha_k \mathrm{D}f_1^k + \alpha_k^2 f_2^k) \quad (14b)$$

$$(1+\sqrt{2}Di\,A_0)\,\mathrm{D}^2T_0 + \sqrt{2}Di\,\mathrm{D}A_0\,\mathrm{D}T_0 = \sum_{k=1}^{K}\mathrm{D}(w_k+T_k) - Di\sum_{k=1}^{K}\mathrm{D}(A_k\,\mathrm{D}T_k) \quad (14c)$$

$$\left[(1+\sqrt{2}Di\,A_0)+\frac{Di}{\sqrt{2}}A_{2k}\right]\mathrm{D}^2T_k - \left[\frac{1}{\sqrt{2}}(w_{2k}-Di\,\mathrm{D}A_{2k}) - \sqrt{2}Di\,\mathrm{D}A_0\right]\mathrm{D}T_k - \left[(1+\sqrt{2}Di\,A_0)\alpha_k^2 - \frac{Di}{\sqrt{2}}A_{2k}\alpha_k^2 + \frac{1}{2\sqrt{2}}\mathrm{D}w_{2k}\right]T_k$$
$$= \frac{1}{\sqrt{2}}\sum_{m=1}^{K}\sum_{n=1}^{K}[(w_n - Di\,\mathrm{D}A_n)\mathrm{D}T_m + Di(\alpha_m^2 T_m - \mathrm{D}^2T_m)A_n]I_2(k,n,m) + \frac{1}{\sqrt{2}}\sum_{m=1}^{K}\sum_{n=1}^{K}\left(\frac{m}{n}\mathrm{D}w_n - Di\,\alpha_n\alpha_m A_n\right)T_m I_1(n,m,k) - Di\,A_k\,\mathrm{D}^2T_0 + (w_k - Di\,\mathrm{D}A_k)\,\mathrm{D}T_0 \quad (14d)$$

where the notation introduced by Georgiadis and Catton [8] is kept. The functionals f_1^k, f_2^k in equation (14b) are the projections of the non-linear terms of the momentum equation (8a) onto mode k

$$f_1^k = \sqrt{2}A_0 v_k + \frac{1}{\sqrt{2}}\sum_{m=1}^{K}\sum_{n=1}^{K} v_n A_m I_1(k,n,m)$$

$$f_2^k = \sqrt{2}A_0 w_k + \frac{1}{\sqrt{2}}\sum_{m=1}^{K}\sum_{n=1}^{K} w_n A_m I_2(k,n,m)$$

and $I_1(k,n,m)$, $I_2(k,n,m)$ are the convolution products defined by Georgiadis and Catton [8] that take the values 1, −1 and 0. The expression for the Nusselt number which represents the net heat transfer across the layer becomes

$$Nu = -\frac{\alpha}{2\pi}\int_0^{2\pi/\alpha}\left[(1+Di|\mathbf{q}|)\frac{\partial T}{\partial z}\right]_{z=0}\mathrm{d}y \simeq -\mathrm{D}T_0(0) - Di\left[\sqrt{2}A_0(0)\,\mathrm{D}T_0(0) + \sum_{k=1}^{K}A_k(0)\,\mathrm{D}T_k(0)\right]. \quad (15)$$

Table 1. Nusselt number convergence of the Fourier expansion (100 z-grid points)

K	Nu	$[Nu_{K=12} - Nu]\times 10^5$
4	1.58659	256
6	1.58870	45
8	1.58904	11
10	1.58913	2
12	1.58915	—

The expression above is equivalent to an L_2 (weak) norm of solution (13).

The $2K+1$ ODEs, equations (14b)–(14d), are approximated with centered finite differences on a uniform grid in the vertical z-direction and solved iteratively. Expansion (13d) is the basic transfer formula for the implementation of a pseudospectral (collocation) scheme that we employ. At each iteration, the Fourier coefficients $A_0, A_1, A_2, \ldots, A_k$ (spectral space) are computed with a discrete Fourier transform after solving equations (14a)–(14b) and evaluating $|\mathbf{q}|$ on a number of equally-spaced points (physical space). At least $2K$ sample points are needed for the Galerkin method to avoid aliasing errors; we performed our computations with 100 sample points per wavelength. The iterations are terminated after the following pointwise-error criterion is satisfied:

$$\max_{1\le k\le K}\max_{0\le z\le 1}\{|w_k^{(i+1)} - w_k^{(i)}|, |T_k^{(i+1)} - T_k^{(i)}|\} < 10^{-6} \quad (16)$$

where (i) is the interation counter. The error tolerance in expression (16) was chosen so that the iteration error is smaller than the truncation error induced by the spectral and finite-difference approximations.

In order to check the accuracy and convergence of the numerical scheme as outlined above, we solve equations (14) for the sample case $Ra_m = 72$, $\omega\,Da = 0.0432$, $Di = 0.2312$, $\alpha = \pi$ which corresponds to the air-saturated bed with 3 layers of polypropylene beads (Section 5). Firstly, we check the convergence of the Fourier series with respect to the weak norm L_2 as represented by the Nusselt number (15). Computations are performed on a uniform z-grid (100 points) for increasing truncation orders K and the results are displayed in Table 1. As K increases, Nu converges at a fast exponential rate. Secondly, tests of Nu and pointwise convergence of the finite-difference scheme are performed by decreasing the mesh size across the layer for constant $K = 6$ (Table 2). The

Table 2. Nusselt number and pointwise convergence of the centered finite-difference scheme for $K = 6$

z-Grid points	Nu	$T_1(0.4)\times 10^2$	$w_1(0.4)$
25	1.59709	6.5532	2.150307
50	1.59070	6.5185	2.138275
100	1.58870	6.5089	2.134932
200	1.58811	6.5063	2.134051

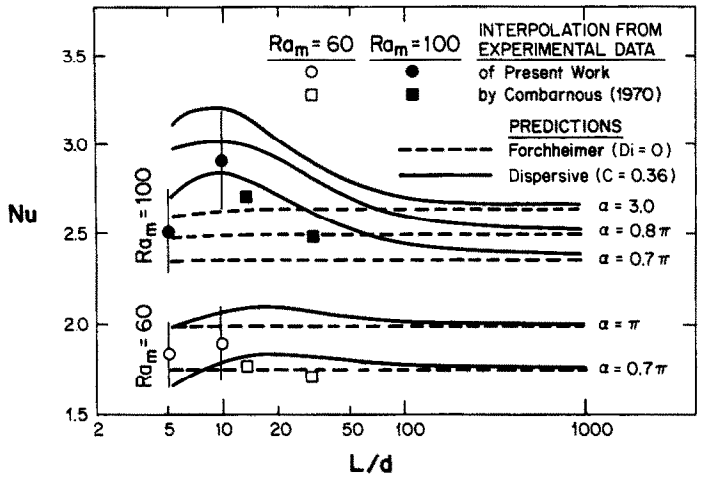

FIG. 3. Heat transport in water-saturated beds of glass beads: dispersion effects for high L/d values.

results demonstrate that the finite-difference scheme converges at a quadratic rate as the mesh size decreases. This is the theoretical convergence rate for the second-order (centered) difference approximations that we employed. The computations reported in the next section are performed with a mesh size of 0.01 (100 z-grid points) and $K = 6$ Fourier modes in expansion (14).

5. NUMERICAL RESULTS AND COMPARISON WITH MEASUREMENTS

The first case to be considered is that of a water-saturated bed of glass beads. Steady-state heat transfer measurements were performed by the authors in a convection cell of rectangular cross-section of dimensions 0.125×0.152 m randomly packed with glass beads of diameter $d = 6$ mm and saturated with distilled water. The experimental procedure used is similar to the one presented by Jonsson and Catton [9]. In our calculations, we use the values of porosity $\phi = 0.394$, stagnant conductivity $k_m = 1.1$ W m^{-1} K^{-1} and permeability $\gamma = 3.7 \times 10^{-8}$ m^2 which have been measured by Jonsson and Catton [9] for the same water-saturated glass beads. Using tabulated data for distilled water at a mean temperature of 13°C, we obtain $Pr_m = 4.5$ and the rest of the input parameters are calculated from equations (5) and (7) with $C = 0.36$.

In Fig. 3, we present the predicted values of the Nusselt number for $Ra_m = 60$ and 100 and the following parameter ranges:

$$5.25 \leqslant L/d \leqslant 1050$$

$$4.11 \times 10^{-6} \leqslant \omega\, Da \leqslant 8.22 \times 10^{-4}$$

$$0.0006 \leqslant Di \leqslant 0.1132.$$

We also plot for comparison the Nusselt numbers obtained by interpolation of the experimental data obtained by the present authors for $L/d = 5$ and 10 and of data reported by Combarnous [2] for $L/d = 13.37$ and 31.5. The error margins shown in Fig. 3 correspond to $\pm 10\%$ error in Nusselt number as estimated by the present authors. The computed Nusselt numbers are obtained for several wave numbers close to the critical. We assume that the selected wave number for each Ra_m does not depend on the parameter L/d. For each wave number, the predicted Nu vs L/d curves show a maximum and approach the Forchheimer model curves ($Di = 0$) asymptotically as $L/d \to \infty$. This trend is justified by the experimental evidence available. There is very little difference between the Nusselt number predictions of the Forchheimer model and the Darcy model ($\omega = Di = 0$), a fact that is expected since the relative importance of the inertial term is expressed by the parameter $\omega\, Da$, which happens to be small in the case above. Note that Nusselt numbers higher than the Darcy predictions can be attained for certain values of L/d only if $Di \neq 0$.

Table 3. Thermophysical data for air-saturated beds of polypropylene beads ($d = 18.4$ mm)

Number of layers	L/d	ϕ	Pr_m	$\omega\, Da \times 10^2$	Di
~ 17	13.37	0.260	0.1484	0.7947	0.0364
5	3.875	0.332	0.1484	3.0366	0.1391
3	2.467	0.369	0.1735	4.3196	0.1735
2	1.761	0.409	0.1919	5.8421	0.3459

The second set of numerical calculations corresponds to the experiments in air-saturated ordered beds of polypropylene beads performed by Close *et al.* [1]. For the cases of 2, 3, and 5 layers, we use the measured values of porosity and stagnant porous medium conductivity given by Close *et al.* [1]. Based on the latter, on thermophysical data for air at a mean temperature of 45°C, and on relations (5) and (7) with $C = 0.36$, the input parameters for the computations are evaluated and presented in Table 3. For the case

Table 4. Numerical predictions of the Nusselt number of the porous Bénard problem (air–polypropylene beds) for the critical wavelength

	Kvernvold and Tyvand [5]	Present work		
Ra_m/Ra_m^c	Darcy	Darcy $Di = \omega = 0$	Forchheimer $Di = 0$	Dispersion $Di = 0.0364$
1.2	1.352	1.353	1.293	1.264
1.6	1.870	1.872	1.767	1.807
1.8	2.072	2.075	1.954	2.052

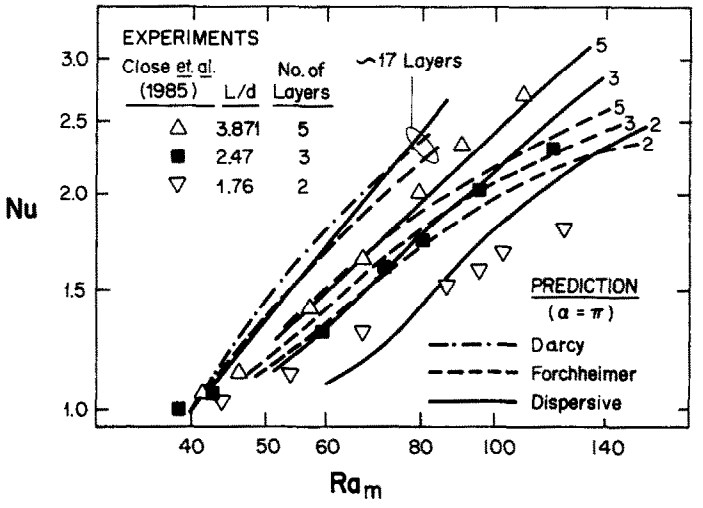

FIG. 4. Effect of the ratio L/d on heat transport in air-saturated beds of polypropylene beads ($d = 18.4$ mm).

$L/d = 13.37$, we assume that the porosity has reached the minimum possible value for the rhombohedral packing (highest density) and that the stagnant conductivity is the same as in the 5 layer case. All the computations are performed for the critical wave number $\alpha^c = \pi$.

In Table 4, we first compare the predictions of the Darcy model ($\omega = Di = 0$), of the Forchheimer model ($Di = 0$), and of the full dispersion model, equations (1)–(4), for the case $L/d = 13.37$ ($\sim$ 17 layers of air-saturated polypropylene beads). The results of our computations for the Darcy–Bénard problem agree very well with the results of Kvernvold and Tyvand [5]. As Fig. 4 shows, dispersion lowers the Nusselt number for low Ra_m values but this trend is reversed as Ra_m increases. The effect of dispersion becomes more dramatic as L/d decreases for 5, 3, and 2 layers of beads; the good agreement with the measurements of Close *et al.* [1] is encouraging. On the other hand, it is evident that the Nusselt number predictions of the Forchheimer model (only inertial effects considered) do not follow the large divergence of the experimental data (Fig. 4). This demonstrates the importance of dispersion on natural convection in shallow (coarse) packed beds.

The following general observations are based on the computed velocity and temperature fields in the porous Bénard problem when the inertia term is small. The inertia effect depends on the magnitude of the porous Prandtl number as we will show in the next paragraph. Dispersion always decreases the mean temperature gradient $DT_0(z)$ (since it augments the effective conductivity of the medium) but the net effect on the total heat transport is more complicated. As $L/d \to \infty$ (e.g. in geophysical porous layers like aquifers and field soils), the velocity and temperature gradient vary very little and thus, according to equations (7) and (15), the net heat transport approaches the Forchheimer limit. As L/d decreases from large to medium values (packed beds found in the laboratory), the velocity and temperature gradient also decrease but Di increases proportionally to d/L; the net effect on the Nusselt number, equation (15), is that it reaches a maximum value and then decreases. It is in this regime of low L/d values that the contribution of the present work becomes apparent. Our results indicate—and this is verified by experiments—that the Nusselt number predicted by the Darcy model cannot be considered as an upper bound on the heat transfer. Although inertia always decreases Nu, dispersion can act to increase or decrease it (Table 4). For natural convection from a vertical plate imbedded in a packed bed, Hong and Tien [11] concluded that dispersion increases Nu. Our numerical solution shows that ther-

Table 5. Numerical predictions of the Nusselt number of the porous Bénard problem (mercury–lead beds) for the critical wavelength and $Ra_m = 60$

			Nu		
L/d	$\omega\, Da$	Di	Darcy $Di = \omega = 0$	Dispersion	Forchheimer $Di = 0$
5.26	0.1782	0.1136	1.7817	1.2039	1.1181
13.15	0.0720	0.0435	1.7817	1.3328	1.3065
26.31	0.0357	0.0226	1.7817	1.4786	1.4654
52.62	0.0178	0.0114	1.7817	1.6027	1.5905
263.1	0.0036	0.0023	1.7817	1.7400	1.7349
2631.0	0.0004	0.0002	1.7817	1.7774	1.7768

mal dispersion can have a stronger effect on the net heat transfer than that of inertia. The latter conclusion was also reached by Cheng and Zheng [10] for mixed convection.

Let us see what happens when inertia becomes as important as dispersion. Based on the governing equations for the porous Bénard problem, equations (2), (3), and (7), the dispersive term is of $O(d/L)$, while the magnitude of the inertia term is $\omega\, Da$ which is of $O(10^{-2} d/L\, Pr_m^{-1})$ when $\phi = 0.4$. Thus, inertia cannot be neglected compared to dispersion when the porous Prandtl number is of $O(10^{-2})$ or less. We report here some numerical results for such a case: convection in a mercury-saturated bed of lead beads with $Pr_m = 0.018$. The thermophysical parameters are given in the experimental work of Jonsson and Catton [9] who reported *Nu* measurements only for one fixed thickness bed with $L/d = 26.31$. In Table 5, we list the numerical prediction of *Nu* as a function of L/d, for $Ra_m = 60$, $\alpha = \pi$. In contrast to the trend of the large Pr_m results of Fig. 3, the function $Nu = Nu(L/d)$ is now monotonic for the Forchheimer/dispersive as well as for the Forchheimer/non-dispersive ($Di = 0$) model. The non-Darcy effects decrease the Nusselt number as the packed bed becomes coarser (low L/d ratio). It is worth noting that this *Nu* decrease is smaller when dispersion is included in the Forchheimer model.

Our computations were confined to low supercritical $Ra_m < 150$ values and no attempt was made to solve the wave number selection problem; the wave number values considered were close to the critical, equations (12). To some extent, our heat transfer results for water-saturated glass beds presented in Fig. 3 complement the predictions of Kvernvold and Tyvand [5]. Using the wave number that maximizes the heat transport, Kvernvold and Tyvand [5] computed the *Nu* vs Ra_m curve for up to $Ra_m \simeq 400$ for water–glass beds. Although their results generally agree with experiments, several points need to be resolved before the validity of their model is justified:

(a) they followed the Nusselt number curve through the inflection point (by solving the two-dimensional steady problem) where the oscillatory regime is known to initiate, cf. Combarnous [2];

(b) the inertial effects were neglected *a priori*;

(c) Kvernvold and Tyvand [5] predicted that dispersion becomes important in a regime where the validity of the dispersion model is questionable.

The small-scale deviations of our predictions from the measurements, see Figs. 3 and 4, can be attributed to the following deficiencies of our model. Firstly, the wave number selection problem was not addressed in this work. It is evident that the wavelength of the convection rolls varies very little after the onset but the Nusselt number depends rather strongly on it. Secondly, although care was taken to use measured values of the thermophysical parameters of the medium, factors such as the medium nonuniformity near the walls and the contribution from radiation were not considered. In the case of very coarse beds (2–3 layers of beads) saturated with air, the aforementioned factors become important especially as far as their influence on the effective conductivity and dispersivity is concerned. In that case, a more refined solution can be obtained by treating the medium as a fluid–solid heterogeneous system and using separate governing equations for the two phases. Nevertheless, the fact that we obtained good agreement between theory and experiments by a continuum approach implies that the introduced homogeneous model remains functional at least for low supercritical Rayleigh numbers.

6. CONCLUSION

A fundamental study of the porous Bénard problem is performed in order to explain some of the large-scale deviations in the Nusselt number measurements found in the literature. Numerical simulations are performed by using a non-Darcian model which includes Forchheimer's extension (inertial term) and the thermal dispersion contribution to the effective conductivity. The predicted Nusselt number results are justified through comparison with measurements, some of which are obtained by the present authors and the rest are reported by Close *et al.* [1] and Combarnous [2]. The good agreement of our predictions with measurements in the range $Ra_m^c < Ra_m \leqslant 150$ suggests the following.

(1) Measured thermophysical data for the fluid–

solid matrix medium should be used when possible. This applies to the values of porosity, permeability, stagnant conductivity and dispersivity.

(2) Dispersion cannot be neglected *a priori* even in natural convection in porous media where the velocities are low unless $d/L \to 0$. In that limit, the Darcian model is a good approximation.

(3) For shallow packed beds, the role of the scale parameter d/L is always important and is manifested both through the dispersive component of conductivity and the inertial (Forchheimer) term. Compared to the predictions of the classical Darcian model, the Nusselt number is decreased for very coarse beds. Dispersion dominates inertia and increases the Nusselt number when d/L is of $O(10^{-1})$ unless the porous medium Prandtl number is of $O(10^{-2})$ or less. In that case, inertia dominates and Nu is decreased.

Acknowledgements—This work was sponsored by the U.S. Department of Energy under grant DE-AT03-82ER12021 (Basic Energy Sciences program). The positive contribution of the reviewers is appreciated.

REFERENCES

1. D. J. Close, J. G. Symons and R. F. White, Convective heat transfer in shallow, gas-filled porous media: experimental investigation, *Int. J. Heat Mass Transfer* **28,** 2371–2378 (1985).
2. M. Combarnous, Convection naturelle et convection mixte dans une couche poreuse horizontale, *Rev. Gen. Therm.* **9,** 1355–1375 (1970).
3. H. Neischloss and G. Dagan, Convective currents in a porous layer heated from below: the influence of hydrodynamic dispersion, *Physics Fluids* **18,** 757–761 (1975).
4. H. Rubin, Thermal convection in a cavernous aquifer, *Water Resour. Res.* **13,** 34–40 (1977).
5. O. Kvernvold and P. Tyvand, Dispersion effects on thermal convection in porous media, *J. Fluid Mech.* **99,** 673–686 (1980).
6. V. Prasad, F. A. Kulacki and M. Keyhani, Natural convection in porous media, *J. Fluid Mech.* **150,** 89–119 (1985).
7. D. J. Close, A general correlation for natural convection in liquid-saturated beds of spheres, *ASME J. Heat Transfer* **108,** 983–985 (1986).
8. J. G. Georgiadis and I. Catton, Prandtl number effect on Bénard convection in porous media, *ASME J. Heat Transfer* **108,** 284–290 (1986).
9. T. Jonsson and I. Catton, Prandtl number dependence of natural convection in porous media, *ASME J. Heat Transfer* **109,** 371–377 (1987).
10. P. Cheng and T. M. Zheng, Mixed convection in the thermal plume above a horizontal line source of heat in a porous medium of infinite extent, *Proc. 8th Int. Heat Transfer Conf.* **5,** 2671–2675 (1986).
11. J. T. Hong and C. L. Tien, Analysis of thermal dispersion effect on vertical-plate natural convection in porous media, *Int. J. Heat Mass Transfer* **30,** 143–150 (1987).
12. J. G. Georgiadis, Numerical study of the inertial effect on natural convection in an infinite horizontal fluid-saturated porous layer, M.Sc. thesis, Engineering, University of California, Los Angeles, California (1984).
13. J. T. Hong, Y. Yamada and C. L. Tien, Effects of non-Darcian and nonuniform porosity on vertical-plate natural convection in porous media, *ASME J. Heat Transfer* **109,** 356–362 (1987).
14. S. Whitaker, Local thermal equilibrium: an application to packed bed catalytic reactor design, *Chem. Engng Sci.* **41,** 2029–2039 (1986).
15. J. G. Georgiadis and I. Catton, An effective equation governing convective transport in porous media, *ASME J. Heat Transfer* (1988), in press.
16. J. G. Georgiadis and I. Catton, Stochastic modeling of unidirectional fluid transport in uniform and random packed beds, *Physics Fluids* **30,** 1017–1022 (1987).
17. J. Levec and R. G. Carbonell, Longitudinal and lateral thermal dispersion in packed beds—Part II: comparison between theory and experiment, *A.I.Ch.E. Jl* **31,** 591–602 (1985).
18. P. G. Saffman, Dispersion due to molecular diffusion and macroscopic mixing in flow through a network of capillaries, *J. Fluid Mech.* **7,** 194–208 (1960).
19. D. D. Joseph, *Stability of Fluid Motions*, Vol. 2, Chap. X. Springer, Berlin (1976).
20. D. D. Joseph, Private communication (1986).
21. D. A. Nield and D. D. Joseph, Effects of quadratic drag on convection in a saturated porous medium, *Physics Fluids* **28,** 995–997 (1985).

DISPERSION DANS LA CONVECTION THERMIQUE CELLULAIREA L'INTERIEUR D'UNE COUCHE POREUSE

Résumé—On étudie numériquement et expérimentalement la convection naturelle bidimensionnelle dans des lits fixes horizontaux saturés. Le modèle classique de Darcy est élargi par le terme de Forchheimer (inertiel) et la conductivité thermique effective du milieu est représentée par la somme d'un terme de stagnation et d'un autre de dispersion (hydrodynamique), ce dernier étant proportionnel à l'amplitude de la vitesse locale de filtration. L'analyse de bifurcation du problème de Bénard en milieu poreux, avec termes d'inertie et de dispersion, prouve que les résultats du modèle classique de Darcy sont encore valables au début de la convection avec faible dispersion. Les deux termes sont importants pour la convection permanente dans lits fixes serrés. L'effet de la dispersion sur le nombre de Nusselt est plus grand que celui de l'inertie tant que le nombre de Prandtl du milieu poreux est de l'ordre de 0,01 ou inférieur. Le rapport de l'épaisseur de la couche au diamètre de bille est un paramètre significatif du problème qui peut aider à comprendre quelques résultats expérimentaux contradictoires.

DISPERSION BEIM AUFTRETEN VON KONVEKTION IN ZELLIGEN, PORÖSEN SCHICHTEN

Zusammenfassung—Es wird über numerische und experimentelle Untersuchungen der zweidimensionalen, auftriebsbedingten Konvektion in gesättigten, horizontalen Festbetten berichtet. Das klassische Darcy-Modell wird um den Forchheimer-Term erweitert und die effektive Wärmeleitfähigkeit des Mediums als Summe einer ruhenden und einer hydrodynamischen, dispersiven Komponente, welche proportional zur örtlichen Filtergeschwindigkeits-Amplitude ist, dargestellt. Eine Analyse des Bénard-Problems poröser Medien mit Termen für die Dispersion und die Trägheit zeigt, daß die Ergebnisse des klassischen Darcy-Modells auch beim Einsetzen von Konvektion für schwache Dispersion gültig sind. Beide Terme sind für die stationäre Konvektion in flachen Festbetten von Bedeutung, Der Einfluß der Dispersion auf die Nusselt-Zahl ist stärker als derjenige der Trägheit, falls die Prandtl-Zahl nicht im Bereich von 0,01 oder darunter liegt. Das Verhältnis von Schichtdicke und Korndurchmesser stellt einen wesentlichen Parameter dar, der einige widersprüchliche Versuchsergebnisse zu erklären hilft.

ДИСПЕРСИЯ ПРИ ЯЧЕИСТОЙ ТЕПЛОВОЙ КОНВЕКЦИИ В ПОРИСТЫХ СЛОЯХ

Аннотация—Численно и экспериментально исследуется случай двумерной конвекции, вызванной подъемными сидами, в насыщенных горизонтальных плотых слоях. Классическая модель Дарси, обобщенная на основе инерционного члена Форшхаймера и эффективной теплопроводности среды, представлена в виде суммы застойной и (гидродинамической) дисперсионной составляющих, причем последняя пропорциональна амплитуде локальной скорости фильтрации. Бифуркационный анализ пористой задачи Бенара с дисперсионными и инерционными членами показывает, что результаты, полученные по классической модели Дарси, справедливы при возникновении конвекции в случае слабой дисперсии. Оба члена существенны для сдучая устойчивой конвекции в плотных слоях малой высоты. По сравнению с инерцией влияние дисперсии на число Нуссетльта сильнее при числе Прандтля пористой среды $\leqslant 0{,}01$. Показано, что отношение толщины слоя к характерному размеру является существенным параметром задачи, дающим возможность объясгить некоторую противоречивость экспериментальных данных.